Solid State Science and Technology, Vol. 17, No 2 (2009) 123-132
ISSN 0128-7389

LUMINESCENCE PROPERTIES OF 30SrO-30MgO-40P_2O_5 DOPED WITH Dy_2O_3

Rosli Hussin[1], Dayang Nur Fazliana Abdul Halim[1], Muhammad Shawal Husin[1], Sinin Hamdan[2] and Mohd Nor Md Yusof[1]

[1]*Phosphor Research Group, Department of Physics, Faculty of Science, Universiti Teknologi Malaysia, Skudai, 81310, Johor*

[2]*Department of Mechanical and Manufacturing System, Faculty of Engineering, Universiti Malaysia Sarawak, 94300, Kota Samarahan, Sarawak*

ABSTRACT

This paper reports on the luminescence properties of Dy^{3+} (1.0 mol%) doped 30SrO-30MgO-40P_2O_5, which had been prepared by solid state reaction. The crystalline phases were identified using X-ray diffraction (XRD) and their luminescence properties were studied using excitation and emission spectra obtained from photoluminescence spectroscopy. The results of XRD patterns indicate that the prepared sample contain $Mg_2P_4O_{12}$ and SrMg P_2O_7 crystalline phase. The excitation spectrum of 30SrO-30MgO-40P_2O_5: Dy^{3+} consist many dominant broad bands' center at ~280,310 and 400-600 nm. The broad band excitation spectrum associated with defects and vacancies of host material through two different crystalline phases present in host material. The other feature of sharp peaks is very similar and belongs to Dy^{3+} ions. The observed f-f transitions in the range of 417-475nm correspond to the transitions from $^6H_{15/2}$ to $^4K_{17/2}$ + $^4M_{19/2,\ 21/2}$ + $^4I_{13/2}$ + $^4F_{7/2}$, $^4G_{11/2}$, $^4I_{15/2}$ and $^4F_{9/2}$, in the range of 392nm to $^6P_{3/2}$ + $^6P_{5/2}$, and in the range of 312-370nm to $^4K_{15/2}$, $^6P_{7/2}$ + $^4M_{15/2}$ and $^4I_{11/2}$ respectively. The sharp emission peaks like at 482,465, and 455 nm could be assigned to the transition of $^4F_{9/2}\rightarrow{}^6H_{15/2}$, $^4I_{15/2}\rightarrow{}^6H_{15/2}$ and $^4G_{11/2}\rightarrow{}^6H_{15/2}$ of Dy^{3+} respectively. Dy^{3+} has emissions due to the atomic energy levels of itself and emissions due to the acceptor levels of defect sites formed by Dy^{3+}. In addition, the SrO-MgO-P_2O_5 is found a new self-active luminescent material.

INTRODUCTION

Since the discovery of solid-state lasers, many glassy/crystalline systems (hosts) have been investigated to study the effect of the host on the lasing properties of the rare earth ions. In addition, the wide application in safety indication, emergency lighting, automobile instrument, luminous paint and optical data storage of long afterglow phosphors resulted in increased research in the field. Rare earth elements doped phosphates have been employed as laser materials, luminophors and x-ray storage phosphors. Increasing interest in these materials has been observed since binary and ternary phosphates could be used as laser devices not only in the form of single crystals but also in the form of powder and glass.

Corresponding Author: rbh@dfiz2.fs.utm.my

Solid State Science and Technology, Vol. 17, No 2 (2009) 123-132
ISSN 0128-7389

Over the past several years, phosphors based on phosphate host matrices have become the subject of great interest for an extensive investigation due to their wide applications in lighting and displays with a high quantum efficiency and stability at higher temperatures. As example, $LaPO_4:Tb^{3+}$ has been considered as an excellent commercial green phosphor that has been widely applied in the development of fluorescent lamps, cathode ray tubes, field emission displays and plasma display panels. Accordingly, some research work has been carried out to improve its properties [1,2]. $LaPO_4:Eu^{3+}$ has been identified as another good phosphate phosphor which displays an intense red emission under an ultraviolet (UV) source [3,4]. It is commercially valuable to decrease the crystallization temperature and replace partial expensive lanthanum oxides by relatively cheaper alkali and alkaline earth metal salts with a negligible influence on the photoluminescence properties.

Recently, alkaline earth phosphate doped with rare earth ions has attracted research interests in the field of photoluminescence since they are suitable hosts with high chemical stability, offers better homogeneity and lowers sintering temperature and also can produce plenty of crystal field environments imposed on emission centers. Alkali earth pyrophosphates constitute a wide family, which, to our knowledge, has been little explored, although their biocompatibility is well established [5]. Few studies on europium-doped pyrophosphates have been reported in the literature. Most of them concern pyrophosphates doped with divalent europium ions, whose luminescence occurs in the blue range. Few studies have been devoted to pyrophosphates doped with trivalent europium. Pelova and Grigorov [6] reported the synthesis of europium-doped zirconium pyrophosphate (ZrP_2O_7:Eu) under air atmosphere and at high temperature. After heating at 900^{o}C, only Eu^{3+} ions were observed in zirconium pyrophosphate, whereas after heating at 1100^{o}C, Eu^{2+} ions were detected. The reduction from Eu^{3+} to Eu^{2+} ions thus occurred in zirconium pyrophosphate at high temperature, even under air atmosphere. The transformation became total only under slightly reducing atmosphere.

Rare-earth (RE) ions possess unique optical behaviour when doped into materials and have paved the way for the development of phosphors for different applications. In recent years, studies on REI-doped glasses have gained much interest of researchers for the reason that the particular 4f electronic configuration of RE in varied glass matrixes leads to emissions from ultraviolet to infrared [7,8] with many potential uses including fluorescent lamps, two-dimensional X-ray sensors, solar control devices, solid laser and optical amplifiers, etc. [9–11]. Nowadays, white light-emitting-diodes have emerged as an important class of lighting devices and show high potential for replacement of conventional lighting sources like incandescent and fluorescent lamps, the advantage being their long lifetime, lower energy consumption, higher reliability and environmental-friendly characteristics [12].

Recently, luminescence materials doped with Dy^{3+} have drawn much interest for its white emission. Dy^{3+} with $4f^9$ configuration has complicated f-block energy levels, therefore, various possible transitions between f levels are expected. However, the transitions between these levels are highly selective, and show sharp line spectra [13].

Corresponding Author: rbh@dfiz2.fs.utm.my

The Dy^{3+} is good activator because of two dominated band in the emission spectra and its position depends strongly on the crystal field of the host lattice used [14]. One is the blue bands (480 nm) corresponding to the $^4F_{9/2} \rightarrow {}^6H_{15/2}$ transition and the other is the yellow band (580 nm) ascribed to the $^4F_{9/2} \rightarrow {}^6H_{13/2}$ transition [15,16]. Luminescent materials doped with Dy^{3+} will present white emission by adjusting the yellow to blue intensity ratio value, which can be used as potential white phosphors [17]. Furthermore, the yellow emission of Dy^{3+} $^4F_{9/2} \rightarrow {}^6H_{13/2}$ are hypersensitive with ($\Delta L=2$, $\Delta J=2$), to the local environment, while its blue emission is not. So many researchers have been engaged in the luminescent property of Dy^{3+} in different composition [18]. As for hosts, phosphates have been shown to be useful hosts for rare earth ions to fabricate phosphors emitting a variety of colours [19–23].

In the present work, we report on the photoluminescence properties of Dy^{3+} doped $30SrO\text{-}30MgO\text{-}40P_2O_5$ phosphors. Crystalline phases of prepared phosphor have been synthesized by a conventional solid-state method and their structures have been examined and confirmed by X-ray diffraction (XRD), and photoluminescence spectra of Dy^{3+}.

EXPERIMENTAL

Powder samples of $30SrO\text{-}30MgO\text{-}40P_2O_5$ doped with 1.0 mol% Dy^{3+} was prepared by solid state reaction. The batch mixture (20g) was prepared using raw materials of reagent grade $SrCO_3$, MgO and H_3PO_4 (85% liquid). The corresponding weights of the starting materials were mixed thoroughly in alumina crucible and placed in air in an electric furnace. A three-step melting schedule was employed to minimize volatilization losses of low-melting starting materials as well as to ensure homogeneous mixing of the constituents. At the first step, the temperature was set to 150^{o}C with heating rate of 15.0^{o}C/min, and maintained for 1 h to facilitate evaporation of water released by P_2O_5. The temperature was then raised to 300^{o}C (heating rate 25^{o}C/min) and left for another 1 h to release CO_2. In the third step, the temperature was increased slowly to 900^{o}C with heating rate of 25^{o}C/min and kept there for 4 h in air. The product was cooled to room temperature.

The structures of the crystalline and amorphous prepared samples were analyzed by means of X-ray diffraction measurements (XRD), using powders form. The XRD measurements were carried out with CuK_α radiation operating at 40 kV, 30 mA with Bragg–Brentano geometry at room temperature using Siemens Diffractometer D5000, equipped with diffraction software analysis. Diffraction patterns were collected in the 2-theta (2θ) range from 10 to 80^o, in steps of 0.05^o and 1s counting time per step.

For photoluminescence measurements, LS50B monochromated 150W fluorescent lamp was used as an excitation source. The photoluminescence spectra were obtained using a monochromator equipped with a photomultiplier tube.

Corresponding Author: rbh@dfiz2.fs.utm.my

Solid State Science and Technology, Vol. 17, No 2 (2009) 123-132
ISSN 0128-7389

RESULTS AND DISCUSSION

The X-ray diffraction for powders sample of the 1% Dy^{3+}-doped 30SrO–30MgO–$40P_2O_5$ was measured and showed the crystalline phase is present in this composition as shown in Fig. 1. Nearly all of the peaks can be indexed to the phase of MgP_2O_6 (ICDD no: 70-1803) and $SrMgP_2O_7$ (ICDD no: 49-1027), indicating that the doping ions Dy^{3+} did not form any new phases in the synthesis process. In other words, only two phases of MgP_2O_6 and $SrMgP_2O_7$ phosphors were obtained by solid state reaction under 900°C.

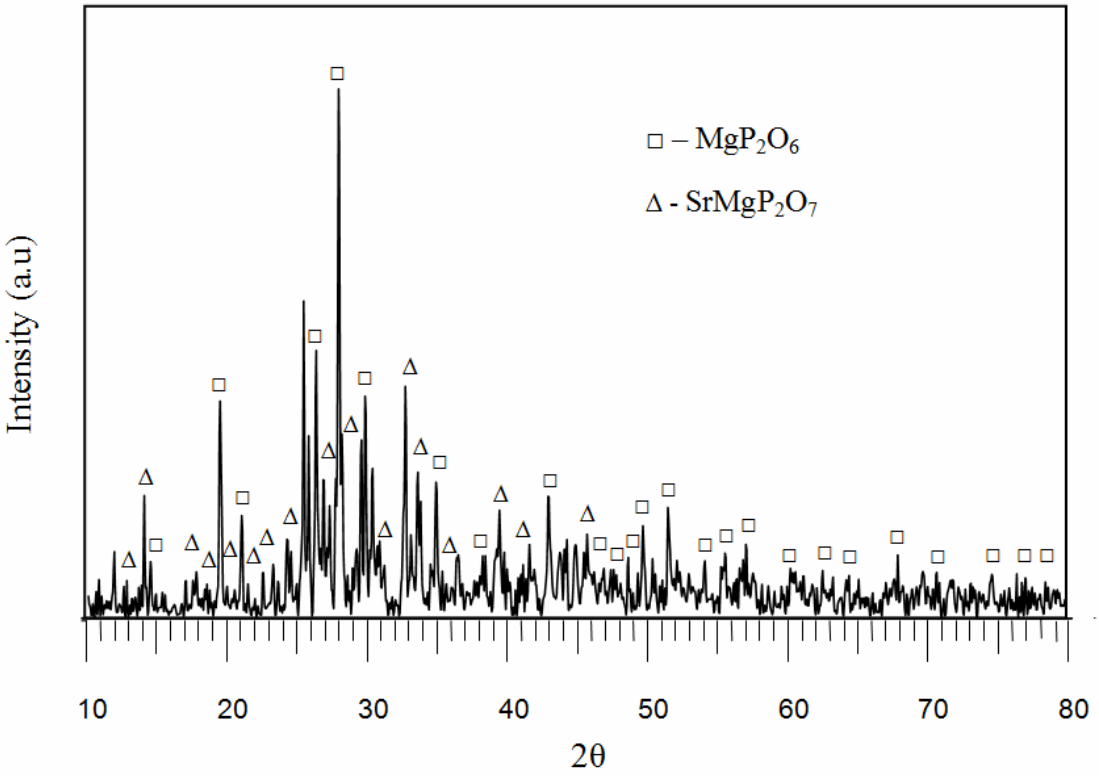

Figure 1: XRD patterns crystalline powder of 1% Dy^{3+} doped 30SrO-30MgO-$40P_2O_5$ sintering at 900°C.

The excitation spectra of powders phosphor sample are shown in Fig. 2. The excitation spectra in the range of in 200–800 nm were measured using conventional fluorescent lamp. The peaks show a large number of broad bands occur during almost coverage UVV range. In the UV range of 200–300 nm, excitation intensity increase evenly with a series of broad band's corresponding to a many extrinsic energy levels in the host matrix or lattice.In this range, the tendency to absorb strongly appears, and there are still some small peaks on the slope. One can see that the broad band ranging in 250-600 nm is much stronger than that in VUV region (~200 nm), contains two strong bands resulting from the f–d transition of Dy^{3+} in the short ultraviolet region (250–300nm) centered at 231,235m, respectively and f–f transition lines within the Dy^{3+} 4f ^{6}

Corresponding Author: rbh@dfiz2.fs.utm.my

Solid State Science and Technology, Vol. 17, No 2 (2009) 123-132
ISSN 0128-7389

configuration in the longer wavelength region (300– 600 nm). This character is very useful for applications of the phosphors absorbing sun light. The assignment of all the bands on excitation is shown on the right part of Fig. 2. Based on this diagram, the excitation spectrum in the range of 312-475nm consists of the f–f transitions of Dy^{3+}: 312 nm ($^6H_{15/2}\rightarrow{}^4K^{15/2}$), 358 nm ($^6H_{15/2}\rightarrow{}^6P_{7/2}+{}^4M_{15/2}$), 370 nm ($^6H_{15/2}\rightarrow{}^4I_{11/2}$), 392 nm ($^6H_{15/2}\rightarrow{}^6P_{3/2}+{}^6P_{5/2}$), 417nm ($^6H_{15/2}\rightarrow{}^4K_{17/2}$ + $^4M_{19/2,\ 21/2}$ + $^4I_{13/2}$ + $^4F_{7/2}$), 455 nm ($^6H_{15/2}\rightarrow{}^4G_{11/2}$), 465 nm ($^6H_{15/2}\rightarrow{}^4I_{15/2}$), 475 nm ($^6H_{15/2}\rightarrow{}^4F_{9/2}$). Comparing the excitation spectra of SrO-MgO-P_2O_5:1% Dy^{3+} (Fig. 2b), and un-doped sample (Fig. 2a), one can see that the excitation lines of Dy^{3+} ions (312, 392, 417 and 475nm) in doped sample are overlapped on the excitation bands of un-doped sample, peaked at 317, 392, 412 and 475 nm. The excitation bands of the un-doped sample may result from the oxygen vacancy due to the reducing bridging oxygen in the phosphate tetrahedral. The broad band can be assigned to the excitations from a localized electron–hole pair, a self trapped excitation (STE), and this broad excitation band also exists in undoped sample [14]. Since this phosphor can efficiently emit composition under the ~200nm excitation range, it is feasible to suggest that this phosphor has a potential application in blue light source.

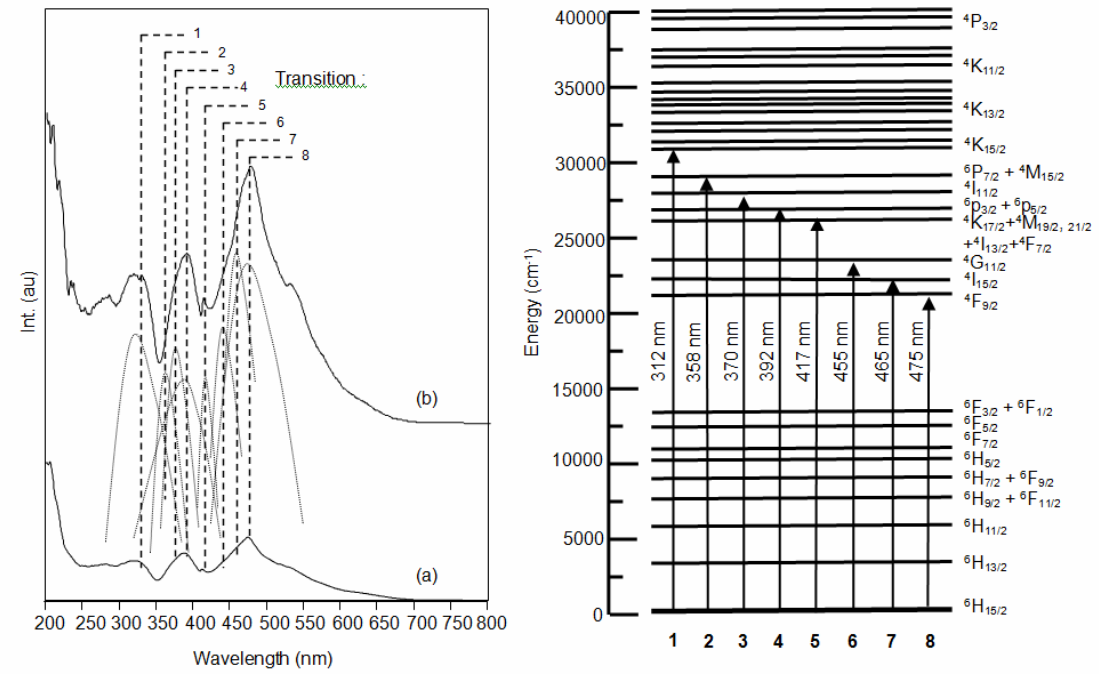

Figure 2: The excitation spectra of 30SrO-30MgO-40P_2O_5, (a) undoped and (b) doped with Dy^{3+} ion. The transitions of the peaks are shown on the right numbered from 1 to 8.

Corresponding Author: rbh@dfiz2.fs.utm.my

Solid State Science and Technology, Vol. 17, No 2 (2009) 123-132
ISSN 0128-7389

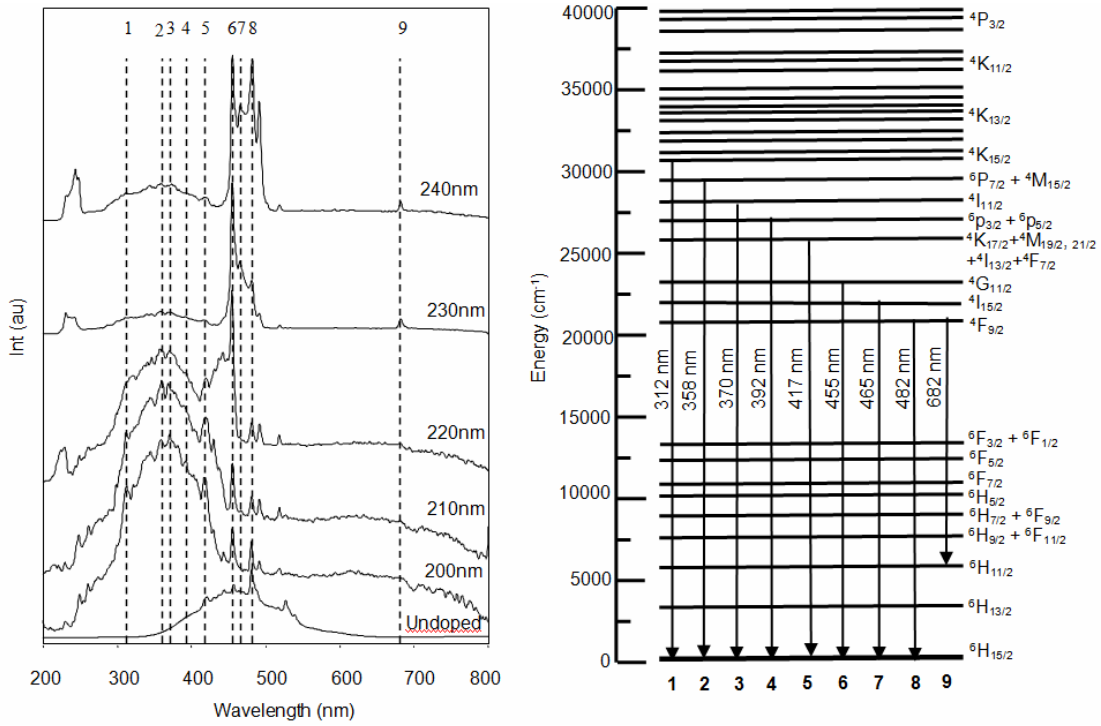

Figure 3: The emission spectrum of 30SrO-30MgO-40P_2O_5 with different excitation from 200-240nm. The transition of the bands is shown on the right with numbering from 1 to 9.

The emission spectrum of 1% Dy^{3+}-doped SrO-MgO-P_2O_5 excited from 200 to 240 nm is shown in Fig. 3. The 200 nm excitation gives rise to one group of peaks around 417,455 and 482nm, and a large part of this wide band is found in the range of visible light, which is conforming to the luminescence phenomenon under 254 nm lamps. Similar with excitation spectrum, there are several peaks in the excitation spectrum as well. The emission spectra not only assigned the transition lines of Dy^{3+} from the lowest energy level $^6H_{15/2}$ but also from the higher energy levels ($^4K_{17/2}$ + $^4M_{19/2,21/2}$ + $^4I_{13/2}$ + $^4F_{7/2}$, $^4G_{11/2}$ and $^4I_{15/2}$) of Dy^{3+} are detected with weaker intensity. The upper level $^4F_{9/2}$ is known to decay radiatively to $^6H_{11/2}$ and $^6H_{15/2}$ levels. The transition $^4F_{9/2}\rightarrow{}^6H_{13/2}$ is very weak and does not appear in any case. The location of the emission lines and their assignments are indicated in the energy level diagram of Dy^{3+} ion on the right part of Fig. 3 [27]. Of these, the $^4G_{11/2}\rightarrow{}^6H_{15/2}$ transition was the strongest in intensity compared to the other transitions, which shows the Dy^{3+} in 30SrO–30MgO–40P_2O_5 host lattices is located at a symmetry local site. They are characteristic emissions of Dy^{3+} as luminescence centers.

The high resolution of the spectra in Fig. 3. is due to the smallest slit width (0.01 mm) that can be used in the measurements. Benefiting from this high resolution, two groups of emission lines were resolved: the 482 nm lines corresponding to the $^4F_{9/2}$□$^6H_{15/2}$ transitions of Dy^{3+} ions, which overlap with the broad emission band of host. It is not

Corresponding Author: rbh@dfiz2.fs.utm.my

surprising that the relative intensities of respective lines are different in the two emission spectra because of different local environments of Dy^{3+} ions, which are supposed to occupy the Sr or Mg sites in the hosts. According to the discussion above, it is impossible that these optical phenomena originate from the electron transition between intrinsic orbits, the extrinsic energy levels from defects will therefore play an important role. Considering the novel structures of these compounds, the Sr/Mg ions in phosphate networks easily move, which induce the formation of all kinds of atomic defect such as Sr/Mg interstitial, Sr/Mg vacancy and Sr/Mg Frenkel pair [32]. However, further investigation is in progress in order to obtain more direct evidences.

The luminescent spectra of Dy^{3+} show the presence of emission lines from higher excited states of Dy^{3+} ($^4K_{17/2}$ + $^4M_{19/2,\ 21/2}$ + $^4I_{13/2}$ + $^4F_{7/2}$, $^4G_{11/2}$ and $^4I_{15/2}$). This is attributed to the low vibration energy of the host complexes. The multiphonon relaxation by host complexes is not able to bridge the gaps between the higher energy levels $^4K_{17/2}$ + $^4M_{19/2,\ 21/2}$ + $^4I_{13/2}$ + $^4F_{7/2}$, $^4G_{11/2}$ and $^4I_{15/2}$) and the $^6H_{15/2}$ level of Dy^{3+} completely, resulting in weak emissions from these levels. In silicate and borates, such emissions cannot be detected [34–36]. It was well known that the Dy^{3+} $^4F_{9/2}\rightarrow{}^6H_{13/2}$ transitions are hypersensitive electronic dipole transitions with $\Delta J = 2$, which are greatly affected by the coordination environment. While $^4F_{9/2}\rightarrow{}^6H_{15/2}$ transitions are magnetic dipole transitions with much less sensitive to the coordination environment.

The $^4F_{9/2}\rightarrow{}^6H_{13/2}$ transition is a forced electric dipole transition being allowed only at low symmetries with no inversion centre [33]. When Dy^{3+} is located at low-symmetry local site (without an inversion centre), this emission is often prominent in its emission spectrum. As the radius of Dy^{3+} (1.03Å) is almost the same as that of Sr^{2+} (1.02Å) so Dy^{3+} can easily enter into the four-fold coordination Sr^{3+} sites (without an inversion center). Therefore, situated at such low-symmetry local sites for Dy^{3+} ions, the $^4F_{9/2}\rightarrow{}^6H_{13/2}$ transition emission is prominent in the emission spectra, which is not observed in emission spectra Fig. 4. In our opinion, Dy^{3+} in the aluminates and silicates act as traps, meanwhile Dy^{3+} in MgP_2O_6 and $SrMgP_2O_7$ crystalline can also act as luminescent centers.

As is shown in Fig.3, the emission spectrum exhibits a blue emission band beside the 358 nm band emission of host, which is similar to the reported $ZnGa_2O_4$ phosphor [33]. In order to explain the blue emission and the 358 nm excitation peak, the undoped sample was also synthesized, its photoluminescence revealed that the 358 nm excitation peak exists in the undoped while monitoring the blue emission, indicating that the 358 nm excitation peaks belong to the host absorption, while the weak blue emission band of doped matrix can be obtained when excited by the 358 nm. It is feasible to suggest that the $SrO\text{-}MgO\text{-}P_2O_5$ is a new self-active luminescent material, as well as the $ZnGa_2O_4$ reported previously [33-36].

Corresponding Author: rbh@dfiz2.fs.utm.my

Solid State Science and Technology, Vol. 17, No 2 (2009) 123-132
ISSN 0128-7389

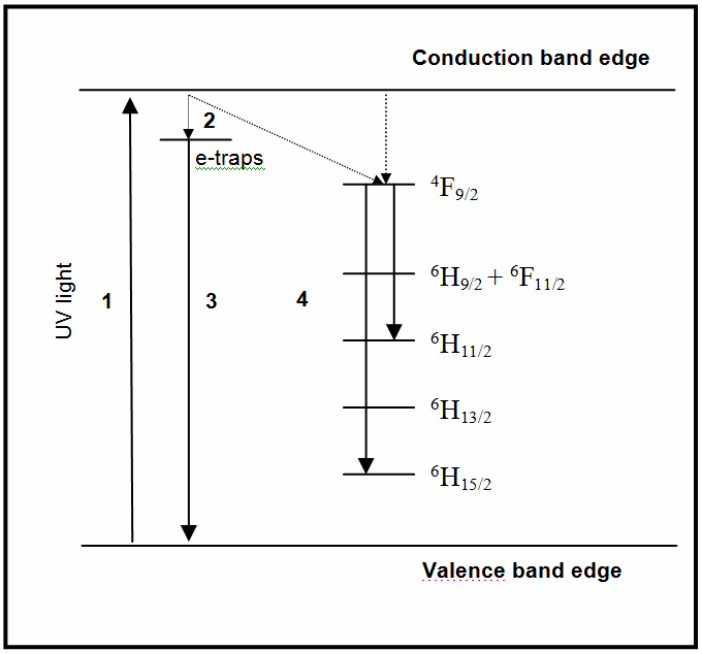

Figure 4: The possible process of the origin of the luminescence in the 30SrO-30MgO-$40P_2O_5$: Dy^{3+} phosphor.

It is clear from the photoluminescence spectra that in the Dy^{3+} doped phosphor, energy transfer from the host to the Dy^{3+} activator ions occurs. When illuminated by UV light excitation source, excitation energy is absorbed by the host and created the STE emission (the 358nm broad band), meanwhile, the absorbed energy is transferred to the Dy^{3+} ion and created the typical emissions of Dy^{3+}.

On the basis of the above spectra results, it is reasonable to explained that, when Dy^{3+} doped into $SrMgP_2O_7$ host, due to the chemically nonequivalent substitution, Dy^{3+} ions act as a role of creating the electron traps during the high temperature synthesis process; the long-lasting phosphorescence originates energy transfer from the electron traps to the Dy^{3+} ions, which give birth to the characteristic emissions of Dy^{3+}. The possible process can be displayed in Fig.4. After irradiation by UV light, the electrons in the valence band are excited to the conduction band and free electrons and holes are formed in the sample host. The holes or electrons were trapped by defect centers, released by heat at room temperature, and recombined with electrons or holes trapped by other defect centers (step 1). One part of the excited electrons returned to the electron traps by the nonradiative way, and got stored in the electron traps which were created at high temperature during the synthesis process (step 2). Because the electron traps are in a metastable state at room temperature, the excited electrons stored in it can be thermally released and be turned back to the valence band edge (step 3). After turning off the excited source, a majority of excited electrons stored in the electron traps would be transferred to the $^4F_{9/2}$ state of Dy^{3+} ions and would create the characteristic emissions of Dy^{3+} ions (step 4). When the decay ratio of the energy transfer from the electron

Corresponding Author: rbh@dfiz2.fs.utm.my

traps to the $^4F_{9/2}$ state of Dy^{3+} ions is proper, the blue light-emitting long-lasting phosphorescence of Dy^{3+} can be obtained.

CONCLUSIONS

Dy^{3+} -doped 30SrO–30MgO–40P_2O_5 crystals were synthesized by solid state method. The experimental results indicate that the role of Dy^{3+} in 30SrO–30MgO–40P_2O_5 is not only the luminescence center, but also a trap center. It is dependent on excitation conditions, including excitation wavelength and intensity. The Dy^{3+} $^4F_{9/2}\rightarrow{}^6H_{15/2}$ transitions are magnetic dipole transitions with much less sensitive to the coordination environment was prominent in the emission spectra, while the hypersensitive $^4F_{9/2}\rightarrow{}^6H_{13/2}$ transition emission was not observed in the emission spectra indicating Dy^{3+} ions located at symmetry local sites. In addition, the SrO-MgO-P_2O_5 is a new self-active material. Therefore, Dy^{3+} ions have potential application for mercury-free blue fluorescence lamp.

ACKNOWLEDGMENTS

We would like to acknowledge the financial supports from Ministry of Science Technology and Innovation (MOSTI) under research grant Project Number: 03-01-06-SF0053, and the authors thank Ibnu Sina Institute, Department of Chemistry, Faculty of Science UTM and Faculty of Mechanical UTM for providing the measurement facilities.

REFERENCES

[1]. I.W. Lenggoro, B. Xia, H. Mizushima, K. Okuyama, N. Kijima, (2001), Mater. Lett. **50,** 92.
[2]. U. Rambabu, D.P. Amalnerkar, B.B. Kale, S. Buddhudu, (2001), Mater. Chem. Phys. **70**, 1.
[3]. R.Y. Wang, (2004), J. Lumin. **106** 211.
[4]. U. Rambabu, S. Buddhudu, (2001), Opt. Mater. **17,** 401.
[5]. J.S. Sun, Y.C. Huang, F.H. Lin, L.T. Chen, (2003), J. Biomed. Mater. Res. Part A **64A** (4) 616.
[6]. V.A. Pelova, L.S. Grigorov, (1997) J. Lumin. **72–74**, 241.
[7]. P.I. Paulose, G. Jose, V. Thomas, et al., (2003) J. Phys. Chem. Solids **64,** 841.
[8]. M. Nogami, T. Enomoto, T. Hayakawa, (2002), J. Lumin. **97**, 147.
[9]. S.E. Paje, M.A. Garcia, M.A. Villegas, et al., (2001) Opt. Mater. **17**, 459.
[10]. Y.P. Reddy, S. Buddhudu, N.S. Hussain, (2001) Mater. Res. Bull. **36**, 1813.
[11]. Y. Lin, Z. Tang, Z. Zhang, J. Zhang, et al., (2001), Mater. Sci. Eng. B **86**, 79.
[12]. C. Zhu, Y. Yang, G. Chen, et al., in: Proceedings of the Ninth International Conference on Particle Physics, October 2005, Como, Italy.
[13]. H. Choi, Ch.H. Kim, Ch.H. Pyun, S.J. Kim, (1999), J. Lumin. **82**, 25.
[14]. G. Blasse, B.C. Grabmaier, 1994, Luminescence Materials, Springer–Verlag, Berlin,

Corresponding Author: rbh@dfiz2.fs.utm.my

[15]. Q. Su, Z.W. Pei, J. Lin, F. Xue, (1995), J. Alloys Compds. **225**, 103.
[16]. J.L. Sommerdijk, A. Bril, (1975), J. Electrochem. Soc. **122**, 952.
[17]. Z. Pei, Q. Su, S. Li, (1991), J. Lumin. **50**, 123.
[18]. Q. Su, J. Lin, B. Li, (1995), J. Alloys Compds. **225**, 120.
[19]. U. Rambabu, S. Buddhudu, (2001), Opt. Mater. **17**, 401.
[20]. R.C. Ropp, (1968), J. Electrochem. Soc. **115**, 841.
[21]. J. Dexpert-Ghys, R. Mauricot, M.D. Faucher, (1996), J. Lumin. **69**, 203.
[22]. X.Q. Su, B. Yan, H.H. Huang, (2005), J. Alloys Compds. **399**, 251.
[23]. B. Yan, X.Q. Su, (2005), Mater. Sci. Eng. B **116**, 196.
[24]. J. Wang, S.B. Wang, Q. Su, (2004), J. Solid State Chem. **177**, 895.
[25]. J. Lin, D.U. Sanger, M. Mennig, et al., (2000), Thin Solid Films **360**, 39.
[26]. J.C. Krupa, I. Gerard, P. Martin, (1992), J. Alloys Compd. **188**, 77.
[27]. E. Cavalli, M. Bettinelli, A. Belletti, A. Speghini, (2002), J. Alloys Compd. **341**, 107.
[28]. M. Yu, J. Lin, Z. Zhang, J. Fu, S. Wang, H.J. Zhang, Y.C. Ham, (2002) Chem. Mater. **14**, 2224.
[29]. X.Q. Zeng, G.Y. Hong, H.Q. You, X.Y. Wu, C.H. Kim, C.H. Pyun, B.Y. Yu, H.S. Bae, C.H. Park, H. Kwon, (2001), Chinese J. Lumin. **22**, 55.
[30]. M. Yu, J. Lin, Z. Wang, J. Fu, S. Wang, H.J. Zhang, Y.C. Han, (2002), Chem. Mater. **14** 2228.
[31]. C.S. Liu, Q. Zhang, N. Kioussis, (2003), Phys. Rev. B **68**, 224.
[32]. L.E. Shea, R.K. Datta, J.J. Brown, Jr., (1994), J. Electrochem. Soc. **141**, 1950.
[33]. T.K. Tran, W. Park, J.W. Tomm, B.K. Wagner, S.M. Jacobsen, C.J. Summers, P.N. Yocom, S.K. McClelland, (1995), J. Appl. Phys. **78**, 5691.
[34]. J.P. Bender, J.F. Wanger, J. Kissick, B.L. Clark, D.A. Keszler, (2002), J. Lumin. **99**, 31.
[35]. F.Y. Chang, L. Pang, (1996), J. Appl. Phys. **79**, 7191.

Corresponding Author: rbh@dfiz2.fs.utm.my